

# We are IntechOpen, the world's leading publisher of Open Access books Built by scientists, for scientists

6,900

Open access books available

186,000

International authors and editors

200M

Downloads

Our authors are among the

154

Countries delivered to

TOP 1%

most cited scientists

12.2%

Contributors from top 500 universities



WEB OF SCIENCE™

Selection of our books indexed in the Book Citation Index  
in Web of Science™ Core Collection (BKCI)

Interested in publishing with us?  
Contact [book.department@intechopen.com](mailto:book.department@intechopen.com)

Numbers displayed above are based on latest data collected.  
For more information visit [www.intechopen.com](http://www.intechopen.com)



# Applications of Fourier Transform Infrared Spectroscopy to Study Cotton Fibers

Noureddine Abidi, Eric Hequet and Luis Cabrales  
*Texas Tech University*  
USA

## 1. Introduction

Fourier Transform Infrared microscopy (FTIR) has become an essential analytical tool available to scientists to study various materials. Specifically FTIR has been increasingly used to study cell wall developments in plants, investigate the efficiency of the surface modification of polymers, identifying contaminants, and predicting the physical properties of certain polymers and biopolymers, etc. This chapter reviews some selected application of the FTIR to study cellulose development in cotton fibers and to predict cotton fiber physical properties. Cotton fiber maturity is a major yield component and an important fiber quality trait that is directly linked to the quantity of cellulose deposited during the secondary cell wall (SCW) biogenesis. Cotton fiber development consists of five major overlapping stages: differentiation, initiation, polar elongation, secondary cell wall development, and maturation. The transition period between 16 and 21 dpa (days post anthesis) is regarded to represent a major developmental stage between the primary cell wall and the SCW. Fourier Transform Infrared spectroscopy was used to investigate the structural changes that occur during the different developmental stages. The IR spectra of fibers harvested at different stages of development (10, 14, 17, 18, 19, 20, 21, 24, 27, 30, 36, 46, and 56 dpa) show the presence of vibrations located at  $1,733\text{ cm}^{-1}$  (C=O stretching originating from esters or amides) and  $1,534\text{ cm}^{-1}$  ( $\text{NH}_2$  deformation corresponding to proteins or amino acids). The results converge towards the conclusion that the transition phase between the primary cell wall and the secondary cell wall occurs between 17 and 18 dpa in fibers from TX19 cultivar, while this transition occurs between 21 and 24 dpa in fibers from TX55 cultivar. The Universal Attenuated Total Reflectance FTIR (UATR-FTIR) was used to evaluate the cotton fiber properties. One hundred and four cotton samples were selected. Thirty FTIR spectra were acquired from each sample and analyzed. Partial Least Square (PLS) analysis of the FTIR spectra was performed and the results showed that microne and surface area (calculated from the AFIS data) could be predicted from the FTIR measurements with very high coefficients of determination. However, the prediction of fiber maturity is probably not possible with the UATR-FTIR. It was concluded that, to be able to predict the fiber maturity with the FTIR, it would be necessary to perform the measurements in the transmission mode rather than in the reflectance mode.

## 2. Fourier transform infrared spectroscopic approach to the study of the secondary cell wall development in cotton fiber

“With kind permission from Springer Science + Business Media: Cellulose, Fourier transform infrared spectroscopic approach to the study of the secondary cell wall development in cotton fiber, 17, 2010, 309-320, Nouredine Abidi, Luis Cabrales, Eric Hequet”.

### 2.1 Introduction

Fiber maturity is a major yield component and an important fiber quality trait that is directly linked to the quantity of cellulose deposited during the Secondary Cell Wall (SCW) biogenesis, and to the organization and orientation of crystalline microfibrils. It is intuitively obvious to hypothesize that immature fibers (having a thin, poorly developed secondary wall) will be fragile, and therefore, are likely to break during the multiple mechanical stresses involved in transforming fibers into yarns. Immature fibers generate short fibers and neps (entanglement of fibers) that result in yarn defects and decreased productivity in the spinning mills. Therefore, studying cotton fiber maturity and understanding the link between SCW biogenesis and cotton fiber maturity is very important. This study was designed to investigate the structural changes occurring during the growth and development of cotton fibers.

Cotton fiber development consists of five major overlapping developmental stages (Wilkin & Jernstedt, 1999): differentiation, initiation, polar elongation, secondary cell wall deposition, and maturation. The day of flowering is referred to as anthesis and the term “days post-anthesis” (dpa) is often used to describe the cotton fiber development. Fiber initiation, which commences at 0 dpa, signals the onset of fiber morphogenesis. Fiber growth is characterized by the synthesis of the primary cell wall and an increase in fiber length up to ~30 mm within 3 weeks after anthesis. The stage of secondary cell wall development commences in general around 21 dpa and continues for a period of ~3 to 6 weeks post-anthesis. This phase is marked by a massive deposition of a thick cellulosic wall (Wilkin & Jernstedt, 1999). The transition period between 16 and 21 dpa is considered to represent a developmental switch in emphasis from primary to secondary cell synthesis during cotton fiber development. During these developmental stages, important structural changes occur leading to cellulose macromolecules formation ( $\beta(1\rightarrow4)$  glucopyranose).

Tokumoto et al. (2002) reported on the changes in the sugar composition and molecular mass distribution of matrix polysaccharides during cotton fiber development. The results showed that the extractable matrix (pectic and hemicellulosic) polysaccharides accounted for 30 - 50% of total sugar content during the elongation stage and less than 3% during the cell thickening stage. With respect to the amount of cellulose present during fiber development, it was reported that the secondary wall thickening and maturation stages are characterized by a dramatic increase in the amount of cellulose (Tokumoto et al., 2002). The primary cell wall was reported to contain between 35 and 50% cellulose (Timpa & Triplett 1993; Meinert & Delmer, 1977). However, the secondary cell wall is composed of nearly 100% cellulose (Haigler et al., 2005).

The composition of the cotton fiber cell wall exhibits a continuous change throughout the development of the fiber (Meinert & Delmer, 1977). Several studies have been focused on

the analysis of the composition of the cell wall extracts (Tokumoto et al., 2002; Timpa & Triplett 1993; Meinert & Delmer 1977; Maltby et al., 1979; Huwlyler et al., 1979, Gokani et al., 1998). However, limited research has been conducted on intact fibers. In previous research, we reported on the usefulness of Fourier Transform Infrared (FTIR) and Thermogravimetric Analysis (TGA) to investigate cotton fiber development (Abidi et al., 2008). The results showed that these two analytical techniques could be used to evaluate the cell wall composition and structure during fiber development. In addition, because of the nondestructive character of the FTIR analysis other testing could be performed on the same set of samples.

Fourier Transform Infrared spectroscopy (FTIR) has emerged as a key technique for the study of plant growth and development (McCann et al., 2007; Yong et al., 2005; Carpita et al., 2001; Zeier & Schreiber, 1999; Chen et al., 1998; McCann et al., 1997; Séné et al., 1994; McCann et al., 1993; McCann et al., 1992). Zeier and Schreiber (1999) used FTIR to characterize isolated endodermal cell walls from plant roots and assigned FTIR frequencies to functional groups present in the cell wall, including the relative amounts of the cell wall biopolymers suberin and lignin, as well as cell wall carbohydrates and proteins. FTIR absorption spectra indicated structural differences for three developmental stages of the endodermal cell wall under study. The authors concluded that FTIR could be used as a direct and non-destructive method suitable for the rapid investigation of isolated plant cell walls. The approach has since been successfully applied to screen large numbers of mutants for a broad range of cell wall phenotypes using FTIR of leaves of *Arabidopsis thaliana* and flax (*Linum usitatissimum*) (Chen et al., 1998). In this study, Chen and co-workers reported that principal component analysis (PCA) of FTIR spectra can distinguish between mutants that are deficient in cell wall sugars. Also, FTIR and Fourier-Transform Raman spectroscopy have been successfully used to investigate the primary cell wall architecture at a molecular level (Séné et al. 1994). Dynamic changes in cell wall composition of hybrid maize coleoptiles (*Zea mays*) were investigated by FTIR (McCann et al., 2007). The authors reported that neural network algorithms could correctly classify infrared spectra from cell walls harvested from individuals differing at one-half-day interval of growth.

The aim of the work reported in this paper has been 2-fold: 1) to investigate the structure and composition of fiber during different phases of development; and 2) to elucidate the effect of cultivar on the developmental stages of the cotton fiber.

## 2.2 Experimental

### 2.2.1 Materials

For this study, two independent replications (10 plants each) of two cotton cultivars (*Gossypium hirsutum* L. cv. TX19 and TX55) were planted in a greenhouse with day/night cycles varying from 13/11 to 11/13 hours and day/night temperatures of about 31°C / 24°C. Plants were grown in 20-L (5 gallons) pots of Sungrow SB 300 potting mix that had been amended with Peters 15-9-12 slow release fertilizer prior to potting. Plants were watered as needed. On the day of flowering (0 dpa), individual flowers were tagged, and 14 developing bolls per cultivar and per replication were harvested at 10, 14, 17, 18, 19, 20, 21, 24, 27, 30, 36, 46, and 56 dpa. The pericarp was immediately removed (excised with scalpel) and isolated ovules were transferred into cryogenic vials and stored in a Cryobiological Storage System filled with liquid nitrogen for analyses. Each replication was tested independently.

## 2.2.2 Methods

### 2.2.2.1 Sample dehydration

Frozen cotton fiber samples were dehydrated using the procedure described in (Abidi et al., 2008; Muller & Jackset al., 1975; Rajasekaran et al., 2006). Frozen samples were first rinsed with water and then washed with acidified solution of 2,2-dimethoxypropane (one drop of HCl in 50 ml of 2,2-dimethoxypropane), followed by five exchanges for 15 minutes each in 100% acetone. In a slightly acidic solution, 2,2-dimethoxypropane is instantly hydrolyzed by water to form methanol and acetone (Muller & Jacks, 1975).

### 2.2.2.2 FTIR measurements

The FTIR spectra of cotton fiber samples were recorded in an environmentally-controlled laboratory maintained at relative humidity of  $65\pm 2\%$  and  $21\pm 1^\circ\text{C}$  using the Spectrum-One equipped with an UATR (Universal Attenuated Total Reflectance) accessory (Perkin-Elmer, USA). The UATR-FTIR was equipped with a ZnSe-Diamond crystal composite that allows collection of FTIR spectra directly on a sample without any special preparation. The instrument is equipped with a "pressure arm" which is used to apply a constant pressure to the cotton samples positioned on top of the ZnSe-Diamond crystal to ensure a good contact between the sample and the incident IR beam and prevent the loss of the IR beam. The amount of pressure applied is monitored by the Perkin-Elmer FTIR software.

Thirty FTIR spectra per sample were acquired for each developmental stage to produce a total of 180 spectra (30 spectra  $\times$  3 replications per dpa  $\times$  2 greenhouse replications). All FTIR spectra were collected at a spectrum resolution of  $4\text{ cm}^{-1}$ , with 32 co-added scans over the range from  $4,000$  to  $650\text{ cm}^{-1}$ . A background scan of clean ZnSe-Diamond crystal was acquired before scanning the samples.

### 2.2.2.3 FTIR spectra analysis

The Perkin-Elmer software was used to perform spectra normalization, baseline corrections, and peak integration. FTIR spectra were then exported to Excel and were subjected to Principal Component Analysis (PCA) with leverage correction and mean-center cross validation boxes checked using Unscrambler V. 9.6 Camo Software AS (CAMO Software AS, Norway).

### 2.2.2.4 Scanning electron microscope

Hitachi Scanning Electron Microscopy (TM-1000, Hitachi Japan) with an accelerating voltage of 15kv was used to visualize the frozen and dehydrated samples. Fibers were placed either on a carbon disc or on a microscopy slide and no coating was performed prior to visualization.

## 2.3 Results and discussion

### 2.3.1 Fourier transform infrared analysis

Figures 1a and b show a series of FTIR spectra of fibers respectively from TX19 and TX55 cultivars during the elongation stage (10, 17, and 19 dpa), during the SCW formation stage (20, 24, and 30 dpa), and during the maturation stage (56 dpa). Compared to the FTIR spectra of mature cotton fibers, several additional vibration bands are noticed in the FTIR spectra of developing cotton fibers.

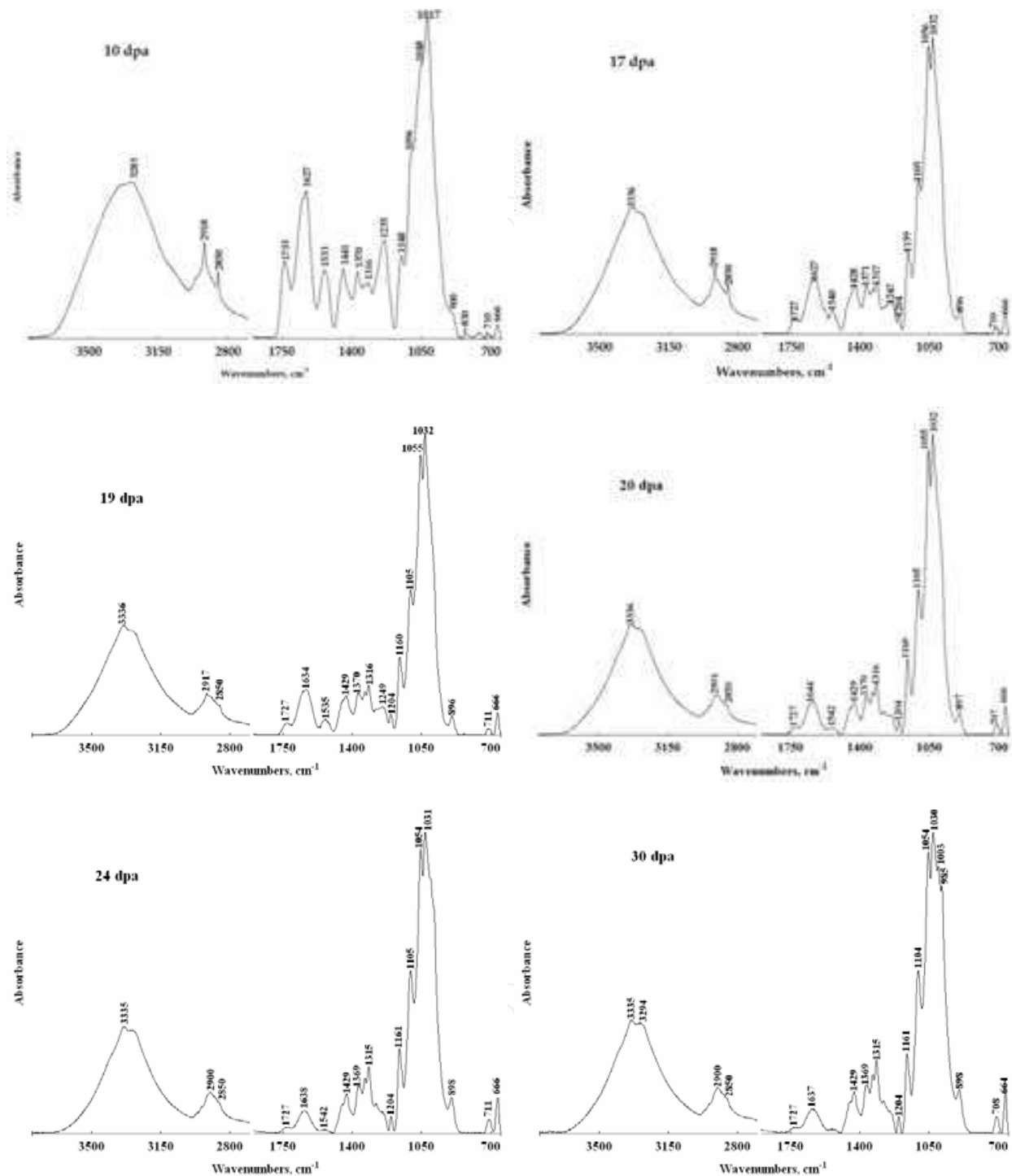


Fig. 1a. FTIR spectra of developing cotton (*Gossypium hirsutum* L. cv. TX19) fibers at different days post-anthesis (dpa)

The vibrations located at 2,918 and 2,850  $\text{cm}^{-1}$  are attributed to  $-\text{CH}_2$  asymmetric vibrations and could originate from the presence of wax substances present on the surface of the primary cell wall (Abidi et al., 2008). The intensities of these two peaks start decreasing at 19 dpa for both cultivars. This result is in agreement with our previous findings (Abidi et al.,

2008). We reported that the percent contribution of the primary cell wall to the total weight of the fiber decreased as wall thickness increases (increased fiber maturity, thus secondary cell wall). Therefore, the relative importance of the vibration bands attributed to noncellulosic substances (e.g. waxes which are located essentially on the primary cell wall) is less.

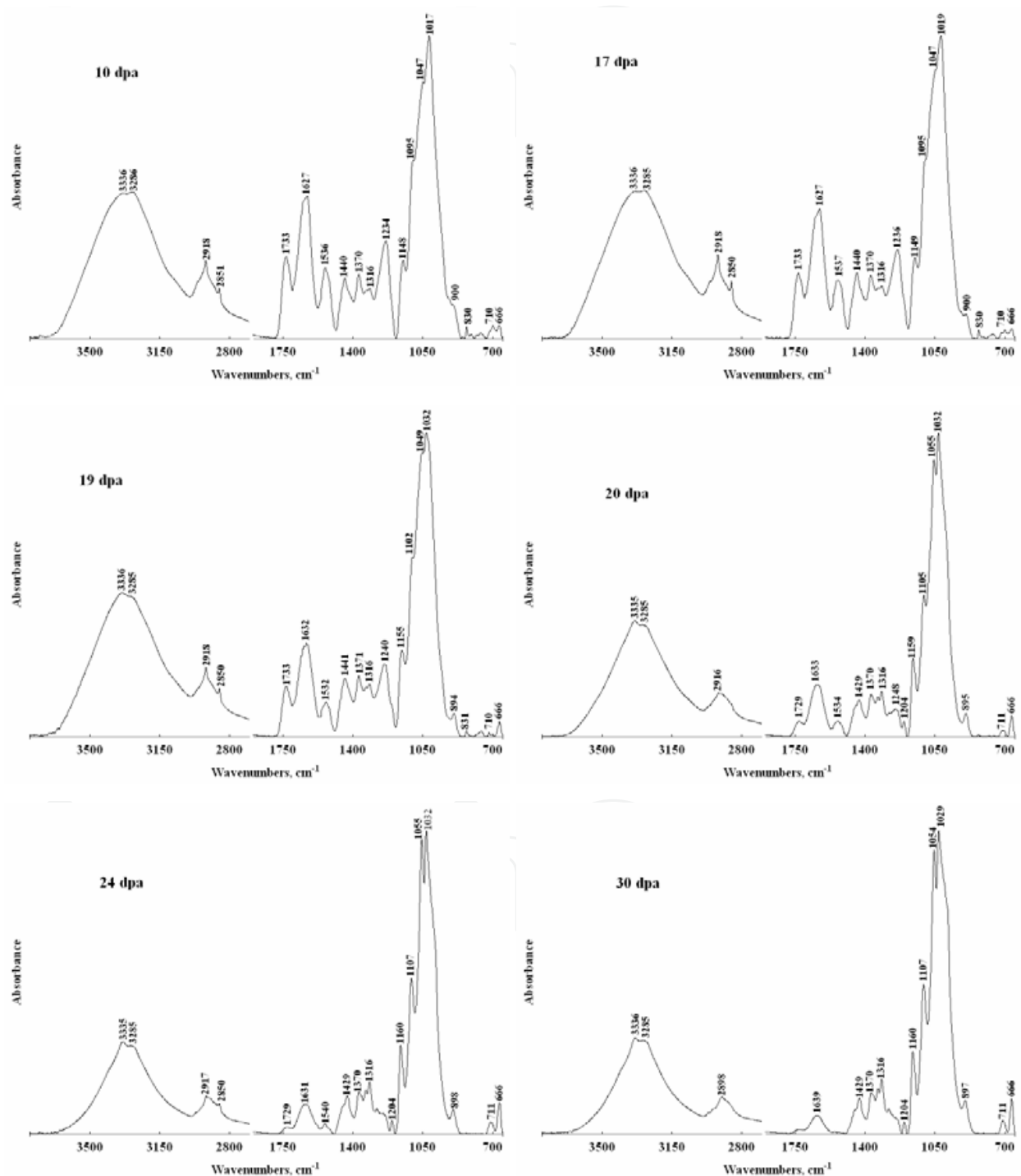


Fig. 1b. FTIR spectra of developing cotton (*Gossypium hirsutum* L. cv. TX55) fibers at different days post-anthesis (dpa)

In addition to O-H bending vibration of water molecules located at  $1,627\text{ cm}^{-1}$ , the FTIR spectra of fibers showed strong absorption between  $3,000\text{ cm}^{-1}$  and  $3,600\text{ cm}^{-1}$  (which is attributed to O-H stretching vibration). This absorption band is composed of two vibrations located at  $3,285\text{ cm}^{-1}$  (attributed to intermolecular hydrogen bonds) and  $3,335\text{ cm}^{-1}$  (attributed to intra-molecular hydrogen bonds) (Liang & Marchessault, 1959). The intensity of the vibration  $3,280\text{ cm}^{-1}$  decreased in the FTIR spectra of fibers older than 17 dpa from TX19 cultivar while for fibers from TX55 the decrease occurred at 19 dpa. The decrease in intensity of  $3,280\text{ cm}^{-1}$  band is associated with an increase in the intensity of the vibration located at  $3,335\text{ cm}^{-1}$ .

The vibration located at  $1,733\text{ cm}^{-1}$  is attributed to C=O stretching vibration and could originate from esters or amides (Abidi et al., 2008). The integrated intensity of this peak ( $I_{1733}$ ) was calculated between  $1,780\text{ cm}^{-1}$  and  $1,701\text{ cm}^{-1}$  and was reported as function of dpa for both cultivars TX19 and TX55 (Fig. 2a). As exhibited in this chart, for fibers from TX19 cultivar  $I_{1733}$  decreased sharply between 10 and 18 dpa and leveled-off at 19 dpa. However, for fibers from TX55 cultivar a continuous decrease is observed between 10 and 24 dpa. The statistical analysis (analysis of variance) showed significant effects of the developmental stage (dpa) and the cultivar on the integrated intensity (Table 1). These results indicate that the structural changes that occur during fiber development are influenced by the cultivar.

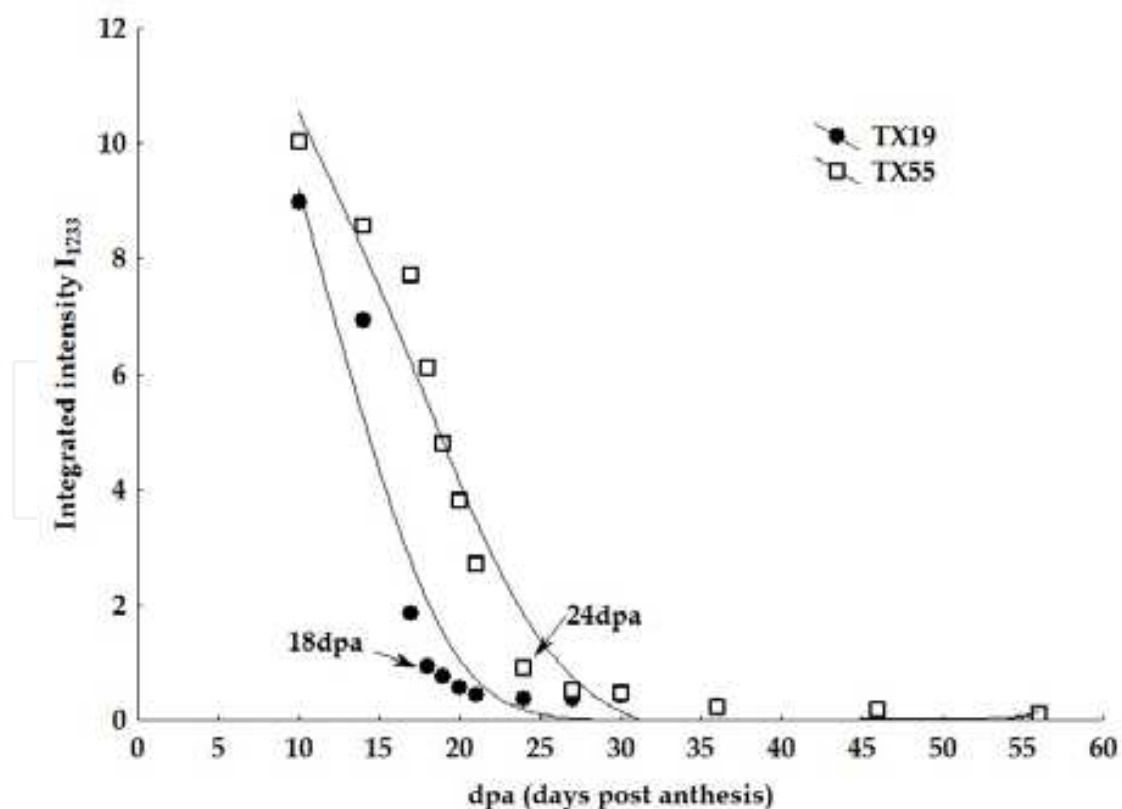


Fig. 2a. Evolution of the integrated peak intensity ( $I_{1733}$ ) as function of developmental stages (dpa)

Parameter	df	F	Probability	Integrated intensity $I_{1733}$ <sup>¥</sup>
<b>Intercept</b>	1	574.4213	0.000001	
<b>Cultivar</b>	1	71.1905	0.000001	
<b>dpa (days post anthesis)</b>	12	60.0900	0.000001	
<b>10</b>				9.5049 a
<b>14</b>				7.7578 b
<b>17</b>				4.7894 c
<b>18</b>				3.5184 d
<b>19</b>				2.7784 de
<b>20</b>				2.1827 de
<b>21</b>				1.5740 ef
<b>24</b>				0.6320 f
<b>27</b>				0.4391 f
<b>30</b>				0.4388 f
<b>36</b>				0.2263 f
<b>46</b>				0.1651 f
<b>56</b>				0.0881 f
<b>Cultivar*dpa</b>	12	7.0895	0.000016	
<b>Error</b>	26			

df, degrees of freedom; F, variance ratio; <sup>¥</sup> Values not followed by the same letter are significantly different with  $\alpha = 5\%$  (according to Newman-Keuls tests).

Table 1. Variance Analysis: Effect of developmental stage (day post-anthesis) and cultivars on the integrated intensity of the peak  $1,733 \text{ cm}^{-1}$  ( $I_{1733}$ )

The vibration located at  $1,627 \text{ cm}^{-1}$  is attributed to O-H bending of adsorbed water molecules (Abidi et al., 2008). The integrated intensity of this peak ( $I_{1627}$ ) was calculated between  $1,701 \text{ cm}^{-1}$  and  $1,576 \text{ cm}^{-1}$ . The change in the integrated intensity  $I_{1627}$  as function of dpa is reported in Fig. 2b for both cultivars. The statistical analysis (analysis of variance) showed a significant effect of the developmental stage and the cultivar on the integrated intensity (Table 2). For fibers from TX19 cultivar, the amount of adsorbed water decreased between 10 and 18 dpa, no significant changes are observed between 19 and 56 dpa. However, for fibers from TX55 cultivar the amount of adsorbed water decreased linearly until the fibers reached 24 dpa. The decrease in the amount of adsorbed water could be attributed to the decrease of the surface area and to reduced accessibility of water molecules to the internal hydroxyl groups to establish hydrogen bonding. This could be the result of increased polymerization reactions of glucose units to form cellulose macromolecules followed by increased crystallinity. Hsieh et al. reported that the degree of crystallinity of two cotton fiber cultivars (Maxxa and SJ-2) increases beginning 24 dpa (Hsieh et al., 1997). The results indicated that the big change in crystallinity occurred between 24 and 28 dpa, and no significant changes occurred thereafter. These results are in agreement with our FTIR results, which indicate that no change in the amount of adsorbed water is noticed between 27 and 56 dpa. In this developmental stage, fibers from both cultivars have nearly the same amount of adsorbed water. This could indicate that the remaining water molecules are those which are strongly bonded to cellulose macromolecules via hydrogen bonding.

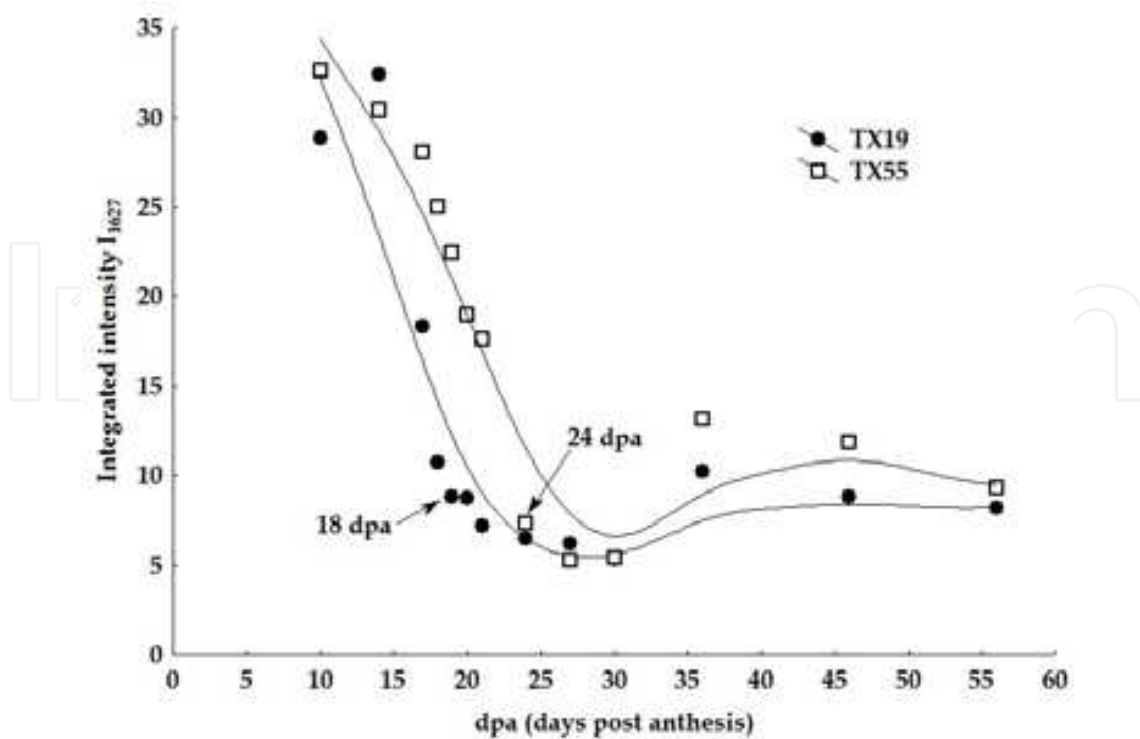


Fig. 2b. Evolution of the integrated peak intensity ( $I_{1627}$ ) as function of developmental stage (dpa)

Parameter	df	F	Probability	Integrated intensity $I_{1627}$ <sup>¥</sup>
<b>Intercept</b>	1	1755.569	0.000001	
<b>Cultivar</b>	1	52.774	0.000001	
<b>dpa (days post anthesis)</b>	12	46.508	0.000001	
10				30.7341 a
14				31.4025 a
17				23.1798 b
18				17.8545 c
19				15.6207 cd
20				13.8401 cde
21				12.3703 ed
24				6.8814 fg
27				5.7146 g
30				5.3511 g
36				11.6973 def
46				10.3251 defg
56				8.7280 efg
<b>Cultivar*dpa</b>	12	4.916	0.000334	
<b>Error</b>	26			

df, degrees of freedom; F, variance ratio, <sup>¥</sup> Values not followed by the same letter are significantly different with  $\alpha = 5\%$  (according to Newman-Keuls tests).

Table 2. Variance Analysis: Effect of developmental stage (day post-anthesis) and cultivars on the integrated intensity of the peak  $1,627\text{ cm}^{-1}$  ( $I_{1627}$ )

The vibration located at  $1,534\text{ cm}^{-1}$  is attributed to  $\text{NH}_2$  deformation and likely indicative of proteins or amino acids (Abidi et al., 2008). The integrated intensity of this peak ( $I_{1534}$ ) was calculated between  $1,575\text{ cm}^{-1}$  and  $1,487\text{ cm}^{-1}$  and the evolution of  $I_{1534}$  as function of dpa for both TX19 and TX55 showed a behavior similar to  $I_{1733}$  (Fig. 2c). An abrupt decrease is observed between 10 and 18 dpa for fibers from TX19 cultivar and a continuous decrease between 10 and 24 dpa for fibers from TX55 cultivar. The statistical analysis (analysis of variance) showed a significant effect of both the developmental stage (dpa) and the cultivar on the integrated intensity (Table 3).

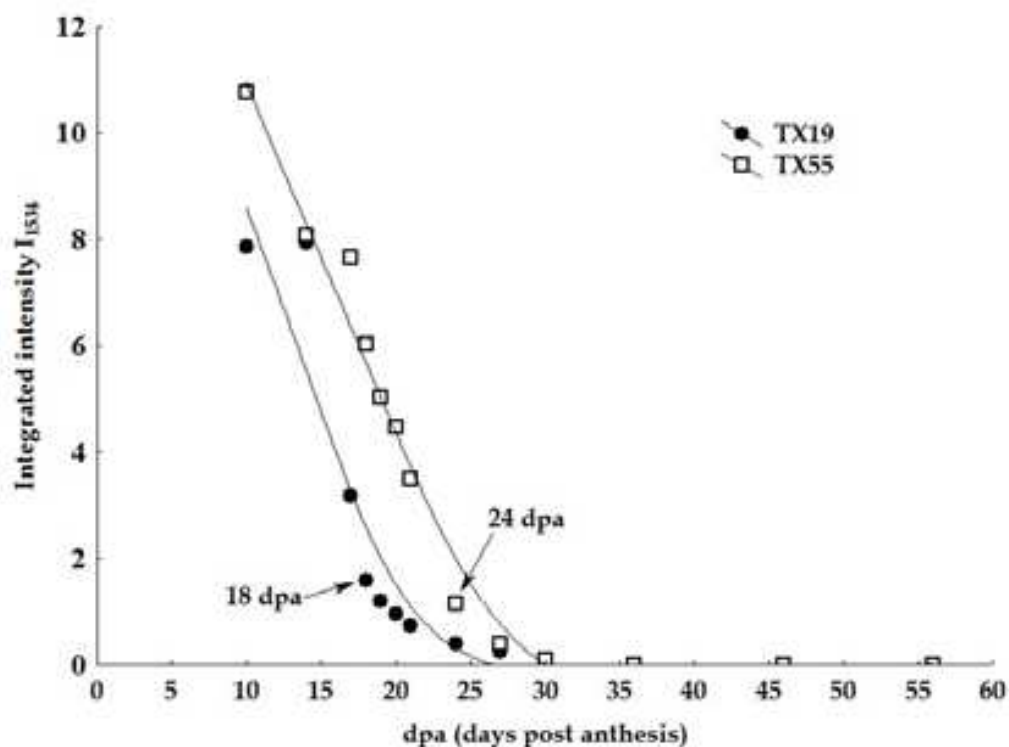


Fig. 2c. Evolution of the integrated peak intensity ( $I_{1534}$ ) as function of developmental stage (dpa)

The vibration located at  $1,236\text{ cm}^{-1}$  is attributed to  $\text{C}=\text{O}$  stretching or  $\text{NH}_2$  deformation (Abidi et al., 2008). This vibration decreased in intensity during fiber development. The disappearance of this band is accompanied by the appearance of a vibration at  $1,204\text{ cm}^{-1}$  at 20 dpa for fibers from TX55 cultivar and as sharp band at 17 dpa for fibers from TX19 cultivar. It is important to point out that the vibration located at  $1,204\text{ cm}^{-1}$  appears only beginning 17 dpa for fibers from TX19 cultivar and beginning 20 dpa for fibers from TX55 cultivar. This vibration has been attributed by Ilharco et al. (1997) to C-O-C stretching mode of the pyranose ring. This vibration appears almost simultaneously with the vibration located at  $900\text{ cm}^{-1}$  (attributed to  $\beta$ -linkage). Consequently, these two vibrations could be considered as the secondary cell wall's fingerprint.

Other vibrations located at  $1,148$ ,  $1,096$ , and  $1,048\text{ cm}^{-1}$  are present only as shoulders in the spectra of fibers from TX19 cultivar at 10 and 14 dpa and become sharper beginning at 17 dpa. It is also noteworthy the shift at 17 dpa of the vibration  $1,148\text{ cm}^{-1}$  to  $1,161\text{ cm}^{-1}$ , the vibration  $1,096\text{ cm}^{-1}$  to  $1,105\text{ cm}^{-1}$ , and the vibration  $1,048\text{ cm}^{-1}$  to  $1,056\text{ cm}^{-1}$ . However, for fibers from TX55 cultivar the shift of these vibrations to higher wavenumbers occurred at 20

dpa. The vibration located at  $1,161\text{ cm}^{-1}$  is assigned to the anti-symmetric bridge C-O-C stretching vibration (Ilharco et al., 1997). The vibration located at  $1,105\text{ cm}^{-1}$  is assigned to anti-symmetric in-plane ring stretching band (Ilharco et al., 1997). The vibration located at  $1,056\text{ cm}^{-1}$  is attributed to C-O stretching mode (Abidi et al., 2008).

Parameter	df	F	Probability	Integrated intensity $I_{1534}$ ¥
<b>Intercept</b>	1	474.3505	0.000001	
<b>Cultivar</b>	1	49.8492	0.000001	
<b>dpa (days post anthesis)</b>	12	48.3051	0.000001	
<b>10</b>				9.3057 a
<b>14</b>				8.0100 a
<b>17</b>				5.4175 b
<b>18</b>				3.8020 c
<b>19</b>				3.1142 c
<b>20</b>				2.7056 c
<b>21</b>				2.1114 c
<b>24</b>				0.7674 d
<b>27</b>				0.3300 d
<b>30</b>				0.0455 d
<b>36</b>				0.0000 d
<b>46</b>				0.0000 d
<b>56</b>				0.0000 d
<b>Cultivar*dpa</b>	12	4.3089	0.000888	
<b>Error</b>	26			

df, degrees of freedom; F, variance ratio, ¥ Values not followed by the same letter are significantly different with  $\alpha = 5\%$  (according to Newman-Keuls tests).

Table 3. Variance Analysis: Effect of developmental stage (day post-anthesis) and cultivars on the integrated peak intensity of the peak  $1,534\text{ cm}^{-1}$  ( $I_{1534}$ )

The vibration located at  $1,017\text{ cm}^{-1}$ , attributed to C-O stretch, is shifted to  $1,031\text{ cm}^{-1}$  at 17 dpa for fibers from TX19 cultivar. However, for fibers from TX55 cultivar, this shift occurs at 19 dpa.

The vibrations located at  $1,003\text{ cm}^{-1}$  and  $985\text{ cm}^{-1}$  appeared at 30 dpa in the spectra of fibers from TX19 cultivar but only at 56 dpa in the spectra of fibers from TX55 cultivar. These vibrations are attributed to C-O and ring stretching modes (Liang & Marchessault, 1959).

The vibration located at  $900\text{ cm}^{-1}$  is attributed to  $\beta$ -linkage (Abidi et al., 2008). This vibration is present only as a small shoulder in the FTIR spectra of fibers from both cultivars at 10 dpa but becomes sharper in the FTIR spectra of fibers from TX19 cultivar at 17 dpa and in the FTIR spectra of fibers from TX55 cultivar at 19 dpa.

The vibration located at  $710\text{ cm}^{-1}$  is attributed to  $\text{CH}_2$  rocking vibration in cellulose  $I_\beta$  (Schwanninger et al., 2004). Using 2D FTIR spectroscopy, Salmén et al. (2005) reported that the peak around  $710\text{ cm}^{-1}$  (which is characteristic of cellulose  $I_\beta$  found in native cotton) has a linear correlation with the percentage of cellulose  $I_\beta$  of the crystalline part. We calculated the peak height of the vibration  $710\text{ cm}^{-1}$  from all FTIR spectra and we reported the data as function of dpa for both genotypes as shown in Fig. 2d. The statistical analysis shows significant effects of the type of cultivar [ $F(1,26)=122.318$ ,  $p=0.000001$ ] and the developmental stage [ $F(12,26)=121.334$ ,  $p=0.00001$ ]. There is also an interaction

developmental stage \* type of cultivar [ $F(12,26)=5.986$ ,  $p=0.00008$ ]. For fibers from TX19 cultivar the peak height of the vibration  $710\text{ cm}^{-1}$  increases linearly between 10 and 30 dpa. No major change is noticed between 30 and 56 dpa. This indicates that the cellulose synthesis during the secondary cell wall development is accompanied by structural organization (increased crystallinity). However, for fibers from TX55 cultivar, the major change of the peak height occurred only beginning 21 dpa. This indicates that for fibers from TX55 cultivar, the structural organization of the cellulose is initiated few days later than in fibers from TX19 cultivar.

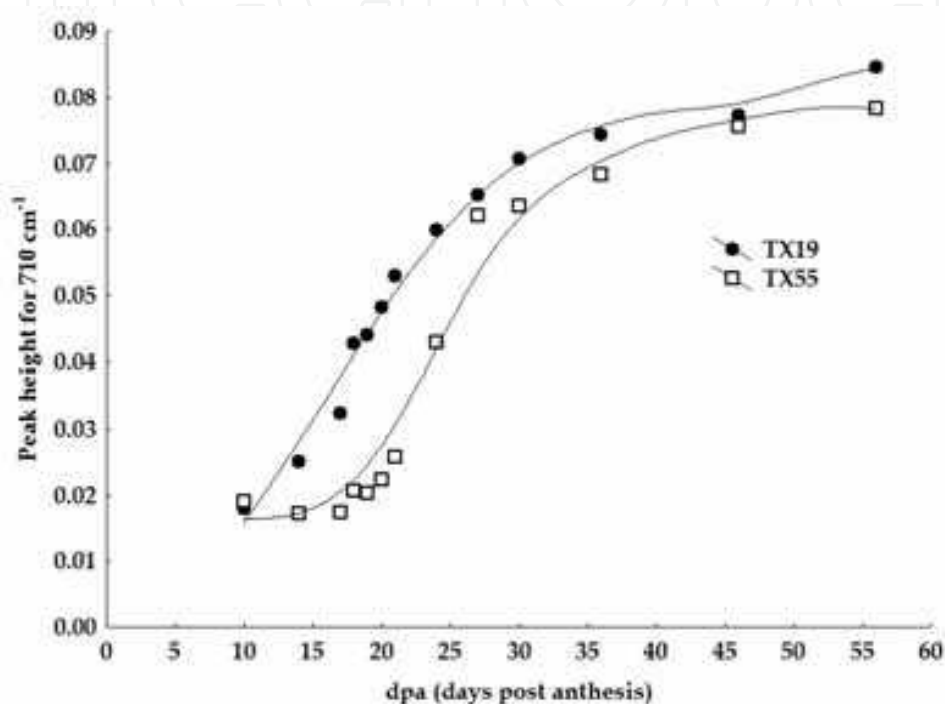


Fig. 2d. Evolution of the peak height for  $710\text{ cm}^{-1}$  as function of developmental stage (dpa)

Figures 2e and f show the relationships between the integrated intensity of the peak  $1,627\text{ cm}^{-1}$  (corresponding to adsorbed water) and the peak height of the vibration  $710\text{ cm}^{-1}$  for fibers from TX19 and TX55, respectively. These relationships show that the decrease of the amount of adsorbed water is associated with an increase in the structural organization of the cellulose (increased crystallinity).

Principal Components Analysis (PCA) was performed on the FTIR spectra in order to identify distinct groups of spectra. The effect of this process is to concentrate the sources of variability in the data into the first 2 PCs (PC1 and PC2). The plots of PC1 against PC2 scores are depicted in Fig. 3a and b, respectively for fibers from TX19 and TX55 cultivars. For fibers from TX19 cultivar, two groups of FTIR spectra could be identified: group 1 includes FTIR spectra of fibers at 10, 14, and 17 dpa; and group 2 includes FTIR spectra of fibers from 18 to 56 dpa. For fibers from TX55 cultivar, two groups of FTIR spectra could also be identified: group 1 includes FTIR spectra of fibers from 10 to 21 dpa and group 2 includes FTIR spectra of fibers from 24 to 56 dpa. It is important to note that the transition between the two groups of FTIR spectra is different for these cultivars: for TX19, the transition occurs at 17 dpa and for TX55 the transition occurs at 21 dpa. Several studies have reported that the transition period between 16 and 21 dpa represents the

developmental switch in emphasis from primary to secondary cell wall synthesis during cotton fiber development (Wilkin & Jernstedt, 1999).

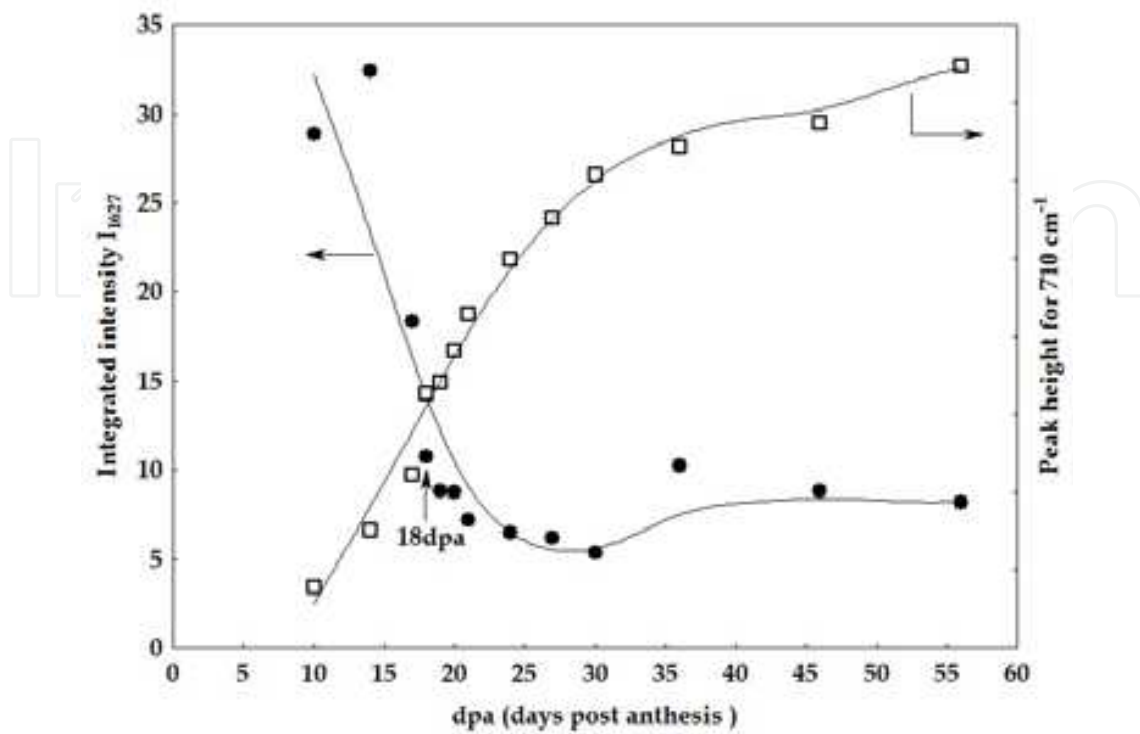


Fig. 2e. Relationship between the integrated peak intensity ( $I_{1627}$ ) and the peak height for 710  $\text{cm}^{-1}$  (*Gossypium hirsutum* L. cv. TX19)

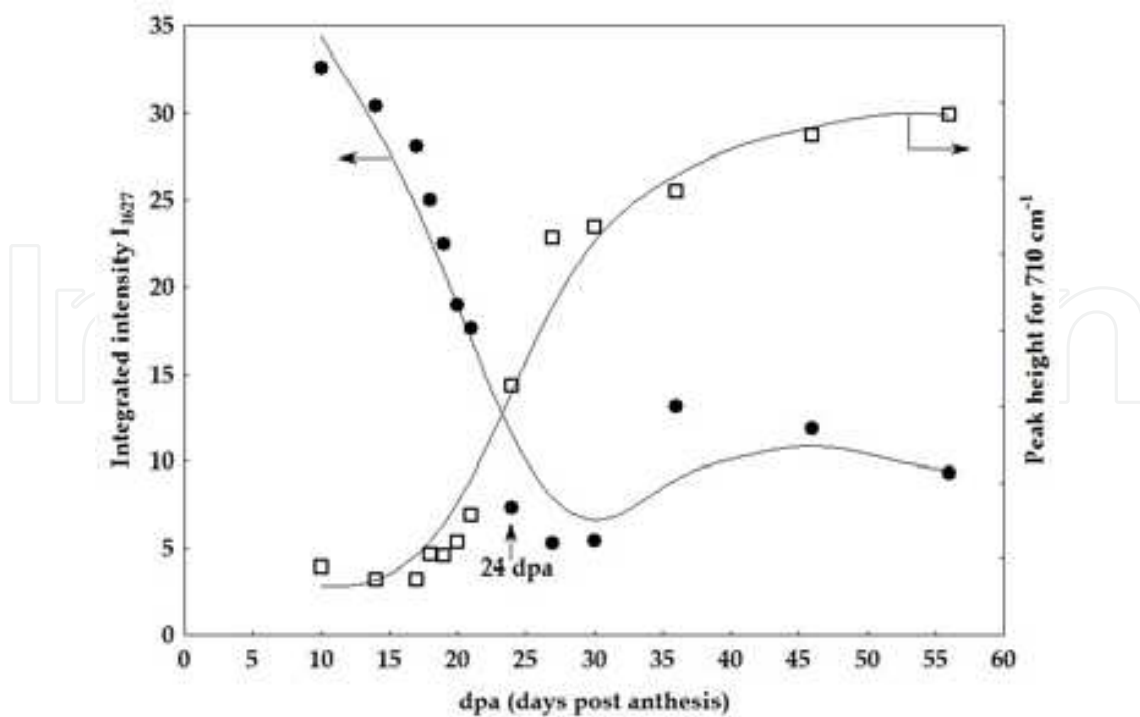


Fig. 2f. Relationship between the integrated peak intensity ( $I_{1627}$ ) and the peak height for 710  $\text{cm}^{-1}$  (*Gossypium hirsutum* L. cv. TX55)

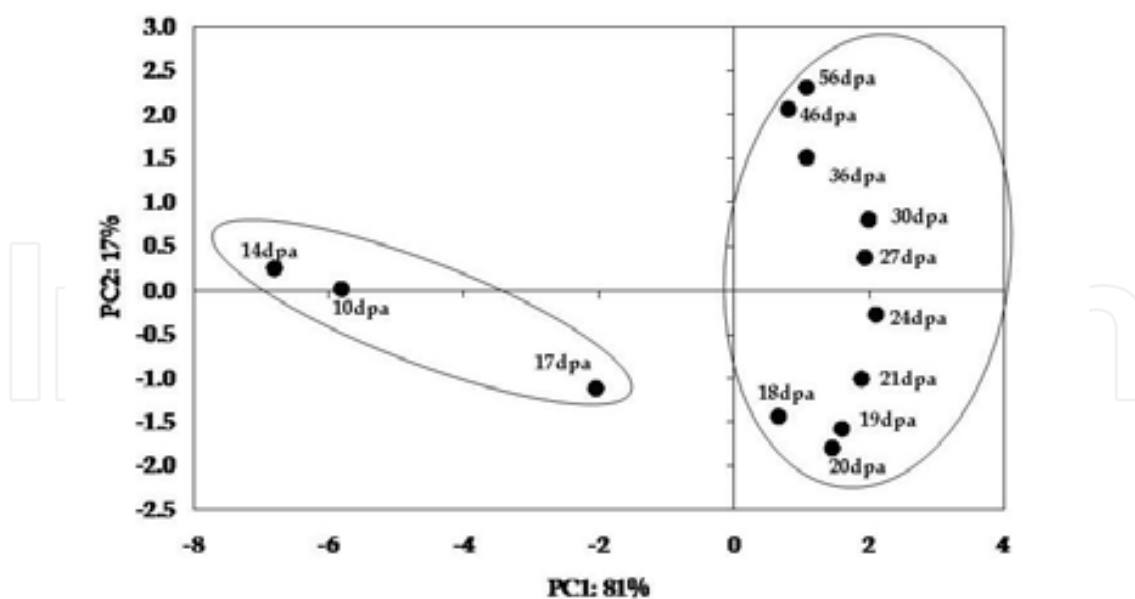


Fig. 3a. Principal Component Analysis of FTIR spectra of fibers from TX19 in the range 4,000 – 650  $\text{cm}^{-1}$

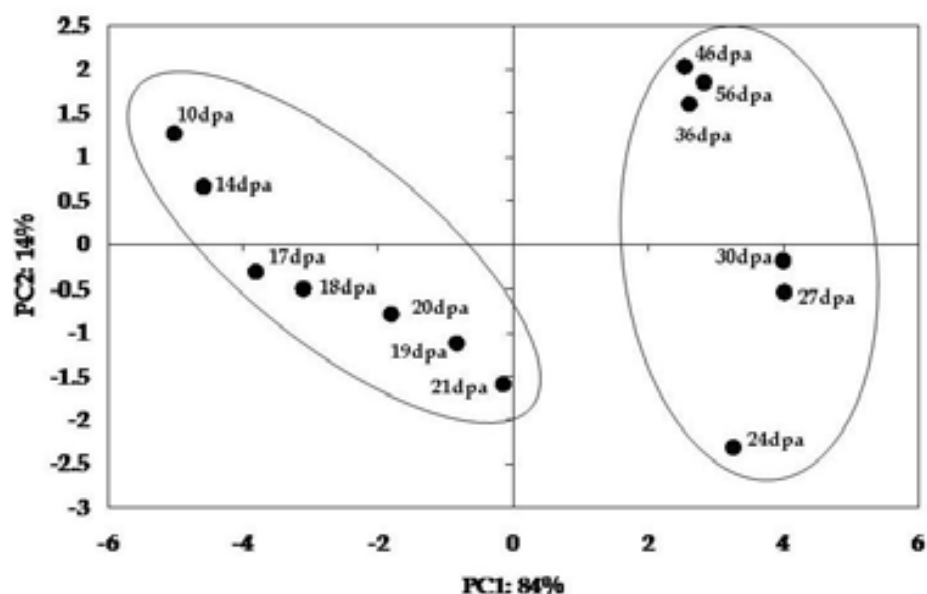


Fig. 3b. Principal Component Analysis of FTIR spectra of fibers from TX55 in the range 4,000 – 650  $\text{cm}^{-1}$

The FTIR data seem to indicate that the secondary cell wall synthesis in fibers from TX19 cultivar could start between 17 and 18 dpa. However, it could start between 21 and 24 dpa in fibers from TX55 cultivar. These data indicate that the FTIR spectroscopy technique has a potential use as screening tool for cotton fiber cultivars that have potentials for early maturation.

### 2.3.2 Scanning electron microscopy

Scanning electron microscopy micrographs of single fibers from selected developing stages are exhibited in Fig. 4. As illustrated in these micrographs, single cotton fibers at 17 dpa

from both cultivars appear transparent consisting mainly of primary cell walls. Single fiber from TX19 at this developmental stage appears slightly thicker than that of TX55. At 20 dpa, fibers from TX19 are thicker than those from TX55, signaling that the secondary cell wall synthesis in TX19 cultivar is well underway at this stage. Fibers from TX55, however, appear thicker only beginning at 24 dpa.

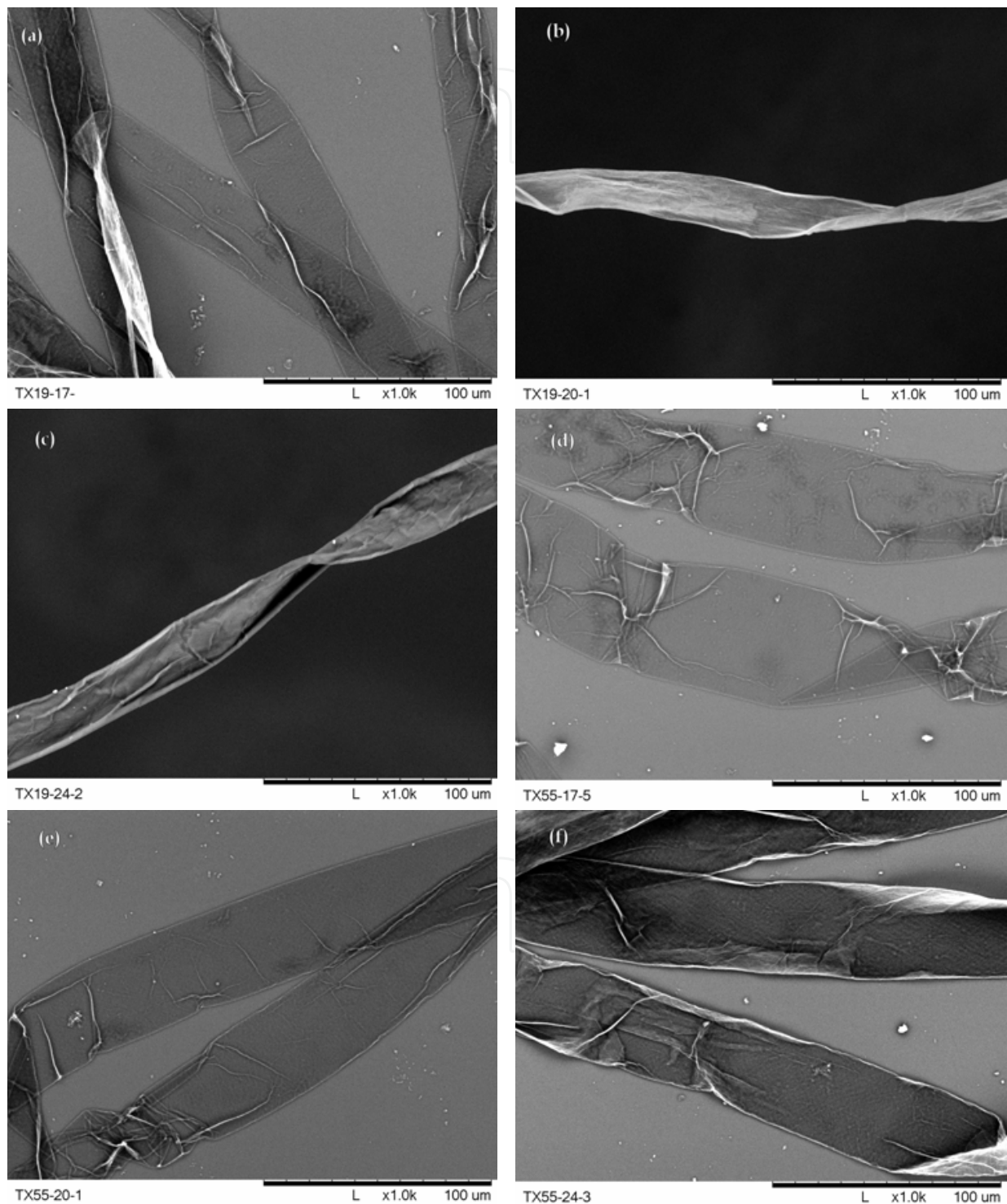


Fig. 4. Scanning electron microscopy micrographs of developing cotton fibers (A) TX19 17 dpa, (B) TX19 20 dpa, (C) TX19 24 dpa, (D) TX55 17 dpa, (E) TX55 20 dpa, (F) TX55 24 dpa

## 2.4 Conclusion

Fourier Transform Infrared spectroscopy was used to investigate the structural changes that occur during cotton fiber development starting at 10 days post-anthesis. FTIR spectra show pronounced differences during fiber development. The evolution of the integrated intensities of specific vibration bands located at 1,733, 1,534, and 1,627  $\text{cm}^{-1}$  as function of developmental stages could be used to monitor the development of the secondary cell wall. FTIR results indicate that the two cultivars investigated (TX19 and TX55) exhibited different structural evolution. The results converge towards the conclusion that the transition phase between the primary cell wall and the secondary cell wall occurs between 17 and 18 dpa in fibers from TX19 cultivar, while this transition occurs between 21 and 24 dpa for fibers from TX55 cultivar. FTIR findings were supported by thermogravimetric characterization of fibers at different stages of development, changes in sugar composition as measured by High Performance Liquid Chromatography, and cellulose content as determined by the anthrone method (data not shown).

## 3. Cotton fiber physical properties prediction using FTIR

### 3.1 Introduction

There is universal interest in measuring cotton fiber properties that are useful to predict the performance of the fiber as an industrial raw material. In addition, significant efforts are being made to develop, through breeding and biotechnology, new cotton varieties that provide superior fiber properties. The “missing link” in these efforts is a scientific understanding of the relationships between the desired properties and the fiber structure/morphology. Among fiber properties, maturity is paramount for several reasons. The effect of maturity on the dye uptake is well known and constitutes the basis of the Goldthwait test (Goldthwait et al., 1947). Similarly, it is known that fine and mature fibers make it possible to spin a finer yarn. But maturity and fineness of cotton fibers are also essential qualitative characteristics if one wants to better understand the propensity of rupture of fibers when they are subjected to stress. It is intuitively obvious to hypothesize that immature fibers (having a thin, poorly developed secondary wall) will be fragile. Thus, they are likely to break during multiple mechanical stresses involved in transforming the fibers from the field to the yarn. These generate short fibers and neps (entanglements of fibers), which will result in yarn defects and decreased productivity.

The dominant tools used today to evaluate fiber properties are the High Volume Instruments (HVI) and the Advanced Fiber Information System (AFIS). The HVI is a fast instrument while the AFIS is relatively slow. Therefore, most of the cotton breeders rely only on HVI measurements. The HVI provides micronaire, length, strength, and color of the lint while the AFIS provides length, maturity, and fineness distributions as well as the nep count and the trash content. While the information provided by the HVI is necessary, it is not sufficient to provide answers about the structure/morphology that are needed to achieve new breakthroughs. The AFIS would be more appropriate but its relatively slow speed and high cost makes it non affordable by most of the cotton breeding programs. In an earlier work, Thermogravimetric Analysis was used to study the relationship between cotton fiber thermal properties and maturity and fineness (Abidi et al., 2007). The results showed that, low micronaires (immature and/or finer fibers), and low maturity ratios (immature fibers) are associated with high weight losses in the region 225 - 425°C. Both low micronaire and low maturity fibers exhibit high surface area for a given weight of fibers.

Therefore, the quantity of the non-cellulosic compounds, mostly present on and in the primary cell wall, is quite large. This leads to higher weight losses in the region 225 - 425°C because in addition to the pyrolysis reactions of cellulose, the decomposition of non-cellulosic compounds also takes place between 225 - 425°C. Furthermore, it was showed that it is possible to estimate the width of the primary cell wall, by comparing the weight losses of two cotton fibers that are identical except for having different maturities (i.e. different degrees of secondary cell wall development).

Our hypothesis is that the FTIR spectroscopy has the potential to assess quickly and accurately some fiber properties related to cotton fiber maturity and fineness. Ramey (1982) used Near-infrared reflectance (NIR) to estimate some quality components of natural fibers. The author explored the use of the NIR to predict the cross-sectional area, the specific surface, micronaire, and causticaire maturity index of cotton fibers. A Neotec Model 41 Grain Quality Analyzer was used to conduct the study. This instrument was equipped with 1.53, 1.97, and 2.32  $\mu\text{m}$  central wavelength filters. The approximate wavelengths for data collection were 1.49 to 1.51, 1.90 to 1.93, 2.16 to 2.19, and 2.26 to 2.30  $\mu\text{m}$ . The author concluded that meaningful estimates of the four mentioned fiber properties could be obtained with near-infrared reflectance. In addition, the author indicated that, except for micronaire, when performing near-infrared reflectance measurements, technician and instrument time per specimen is less than the usual procedures.

Montalvo and Von Hoven (2004) made a comprehensive review on both the reference methods and the application of NIR to predict cotton fiber properties (fineness, maturity, and micronaire). The authors indicated that successful application of NIR spectroscopy to cotton fiber quality measurements has been limited by shortcuts in the development and validation of NIR instruments and methodologies.

In this study, we used the Universal Attenuated Total Reflectance Fourier Transform Infrared (UATR-FTIR) to predict cotton fiber properties. The FTIR spectra were acquired in the mid-infrared range (4,000 - 650  $\text{cm}^{-1}$ ). After baseline correction and spectra normalization, the Partial Least Square was used to predict micronaire, maturity, and surface area.

### 3.2 Materials

One hundred and four cotton bales representing the two principal cultivated species were selected. These cotton samples were the same cotton samples used in our previous study (Hequet et al., 2006). The vast majority of the bales originated in the U.S.A., but some foreign-grown cotton bales were also selected (Egypt, Uzbekistan, Pakistan, Cameroon, Syria, Benin, and Australia). The bales were opened and ten samples per bale were taken. Each sample was tested using a HVI Uster 900A. For each bale, a total of 40 micronaire tests and 100 length and tenacity tests were done. This allowed us to conclude that the intra-bale variability was acceptable and that we had a wide range of fiber properties (Table 4). The same samples were also tested on the AFIS with 5 replications and 3,000 fibers tested per replication. This totaled 150,000 fibers per bale.

A representative sample of approximately 30 kg (70 pounds) was taken from each bale. Each sample was homogenized according to the protocol used by the ICCSC (International Cotton Calibration Standard Committee, 1999 (USDA, 1999) to produce reference cottons. From the card web produced, 20 samples were taken. Samples 1 to 5 were re-sampled (8 pinches per sample). This new sample was delicately mixed manually then 2 fibrograph

combs were formed. We chose to sample with the fibrosampler because this method, unlike Lord's method, is not length biased. This procedure was repeated for samples 6-10, 11-15 and 16-20. A sample was then taken from each of the 8 combs produced. For each comb, a minimum of 500 cross sections were analyzed following the procedure described in (Hequet et al., 2006). When the CV% of the averages between combs was higher than 2%, eight other combs were produced and 500 additional cross sections (per comb) were analyzed. The original CV% was confirmed in almost every case. From this point forward the 104 cottons homogenized according to the ICCS protocol will be called reference cottons.

	<b>Micronaire</b>	<b>UHML (inch)</b>	<b>UI (%)</b>	<b>Tenacity (cN/tex)</b>	<b>Elongation (%)</b>
<b>Average :</b>	4.2	1.08	81.9	29.4	5.4
<b>Minimum</b>	2.6	0.96	78.6	21.6	3.6
<b>Maximum</b>	5.7	1.31	84.5	41.3	8.3
<b>Intra-bale CV% :</b>					
<b>Average</b>	0.7	0.9	0.6	1.9	3.5
<b>Minimum</b>	0.0	0.4	0.2	0.8	1.4
<b>Maximum</b>	2.2	2.2	1.1	3.1	7.7

Table 4. HVI fiber properties of the 104 bales: Basic statistics

### 3.3 Methods

#### 3.3.1 FTIR measurements

Spectrum-One equipped with an UATR (Universal Attenuated Total Reflectance) accessory was used to acquire the FTIR spectra of the cotton fiber samples (PerkinElmer, USA). The UATR-FTIR was equipped with a ZnSe-Diamond crystal composite that allows collecting the FTIR spectra directly on a sample without any special preparation. The FTIR spectrometer was placed in a conditioned laboratory at  $65\pm 2\%$  RH and  $21\pm 1^\circ\text{C}$  and all the FTIR spectra were acquired in this environment. Cotton samples were placed on top of the ZnSe-Diamond crystal and a pressure was applied on the sample to ensure a good contact between the sample and the incident IR beam and to prevent loss of the IR beam. The amount of pressure applied was kept the same and it was monitored through the FTIR software included in the Perkin-Elmer software package. Therefore, all samples were subjected to the same pressure.

A representative sample was taken from each reference cotton. Thirty spectra from each sample were acquired and analyzed. All the FTIR spectra were collected at a spectrum resolution of  $4\text{ cm}^{-1}$ , with 32 co-added scans, over the range of  $4,000 - 650\text{ cm}^{-1}$ . A background scan of clean ZnSe-Diamond crystal was acquired before acquiring the spectra of the sample. The Perkin-Elmer software was used to perform the baseline corrections of the spectra.

### 3.3.2 FTIR spectra analysis

The raw FTIR spectra were normalized (centered and scaled) and averaged. Then, the PLS1 (Partial Least Square) was run with a full cross-validation (The Unscrambler V. 9.6 Camo Software AS, USA). An uncertainty test was performed for each test. Full cross validation means that the same samples are used both for model estimation and testing. One sample is left out from the calibration data set and the model is calibrated on the remaining data points. Then the value for the left-out sample is predicted and the prediction residuals are computed. The process is repeated with another subset of the calibration set, and so on until every sample has been left out once; then all prediction residuals are combined to compute the validation residual variance and RMSEP (Root Mean Square Error of Prediction). RSMEP can be interpreted as the average prediction error. Therefore, we can give the predicted Y-values an estimated precision of two times the RSMEP.

### 3.4 Results and discussion

For each sample in addition to the FTIR measurements, the following fiber properties were selected: HVI micronaire, image analysis of the cross-sections (perimeter and theta), and the AFIS data (calculated Area mm<sup>2</sup>/mg). PLS1 (Partial Least Square) procedure, was used to predict these fiber maturity-related parameters. Partial Least Square regression is a method that relates the variations in one response variable (micronaire for example) to the variations of several predictors (X variables = absorbance for the different wavelengths) with explanatory or predictive purposes. This method performs particularly well when the various X-variables express common information, i.e. when there is a large amount of correlation, or even collinearity between them, which is the case with the FTIR spectra. Partial Least Square regression is a bilinear modeling method where information in the original FTIR data is projected onto a small number of underlying ("latent") variables called PLS components. The Y-data are actively used in estimating the "latent" variables to ensure that the first components are those that are most relevant for predicting the Y-variables. Interpretation of the relationship between X-data and Y-data is then simplified as this relationship is concentrated on the smallest possible number of components.

#### 3.4.1 Prediction of the micronaire

Cotton fiber micronaire is a function of fineness and maturity. It is based on the measurement of an air flow that passes through a porous plug of cotton fibers. The micronaire is proportional to the inverse of the specific surface of the cotton fibers. It should be noted that the definition of fiber fineness in cotton does not relate directly to fiber perimeter. Indeed, fiber fineness (expressed in millitex) is the weight in mg of 1,000 meters of fibers. Therefore a fine fiber may have a small perimeter and a high maturity ratio. Conversely, a fine fiber may have a large fiber perimeter and a low maturity ratio (which implies a large lumen in the fiber). In a similar manner, high micronaire readings indicate coarse fibers (high weight per unit length), while low micronaire readings indicate fine fibers (low weight per unit length).

Figure 5a shows the relationship between the FTIR and the HVI micronaire. With a coefficient of determination of 0.9252, the FTIR measurements lead to very good prediction of the micronaire (FTIR prediction = 0.9253\*Micronaire + 0.3349). It should be noted that the coefficient of determination of the validation ( $R^2 = 0.8677$ ) set is nearly as good as the coefficient of determination of the calibration set (fig. 5b).

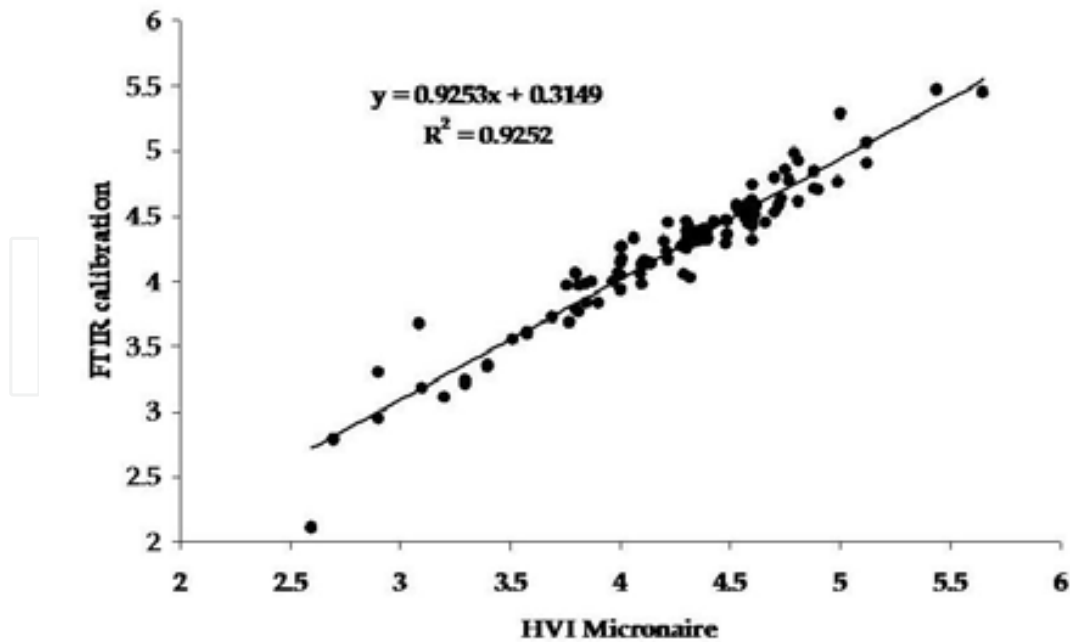


Fig. 5a. FTIR HVI micronaire prediction (calibration) versus HVI micronaire

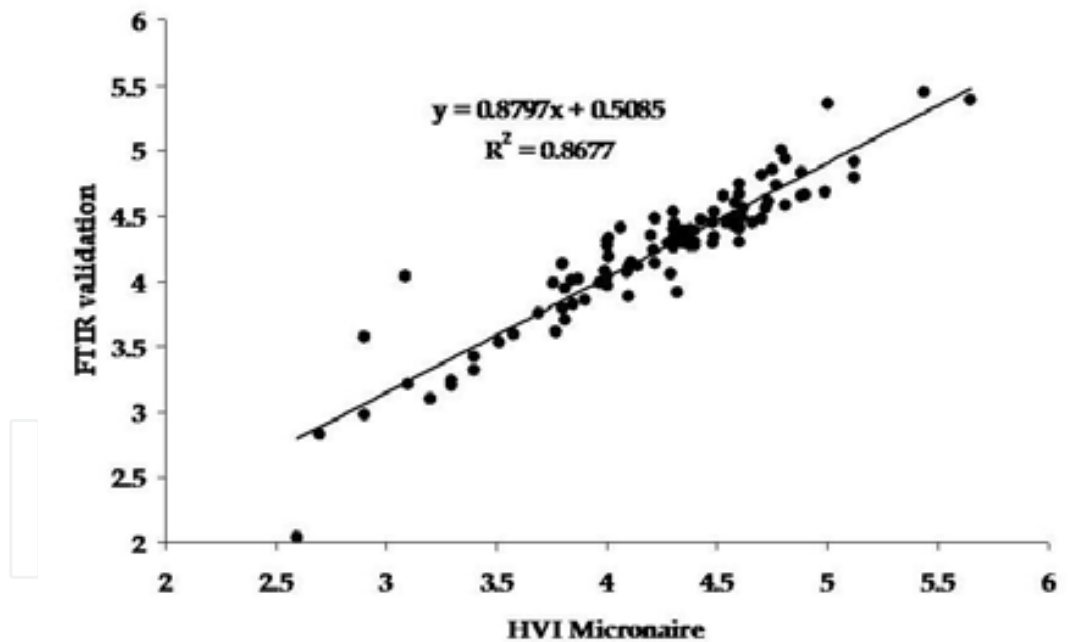


Fig. 5b. FTIR HVI micronaire prediction (validation) versus HVI micronaire

### 3.4.2 Prediction of fiber perimeter and theta

Fiber perimeter and theta were determined by image analysis (Hequet et al., 2006). Theta, degree of secondary cell wall thickening, is defined as the ratio of the area of the cell wall to the area of a circle having the same perimeter as the fiber cross-section. The measurement of theta leads to the determination of the maturity ratio  $M$  ( $\theta = M \cdot 0.577$ ). Figure 6a shows the prediction of the fiber perimeter with FTIR (FTIR prediction =  $0.6529 \cdot \text{Perimeter} + 18.308$ ).

The coefficient of determination ( $R^2 = 0.6529$ ) of the calibration set is not very good. For the validation set, the coefficient of determination ( $R^2 = 0.4548$ ) is much lower (Fig. 6b). These results reveal that the PLS1 model is not valid.

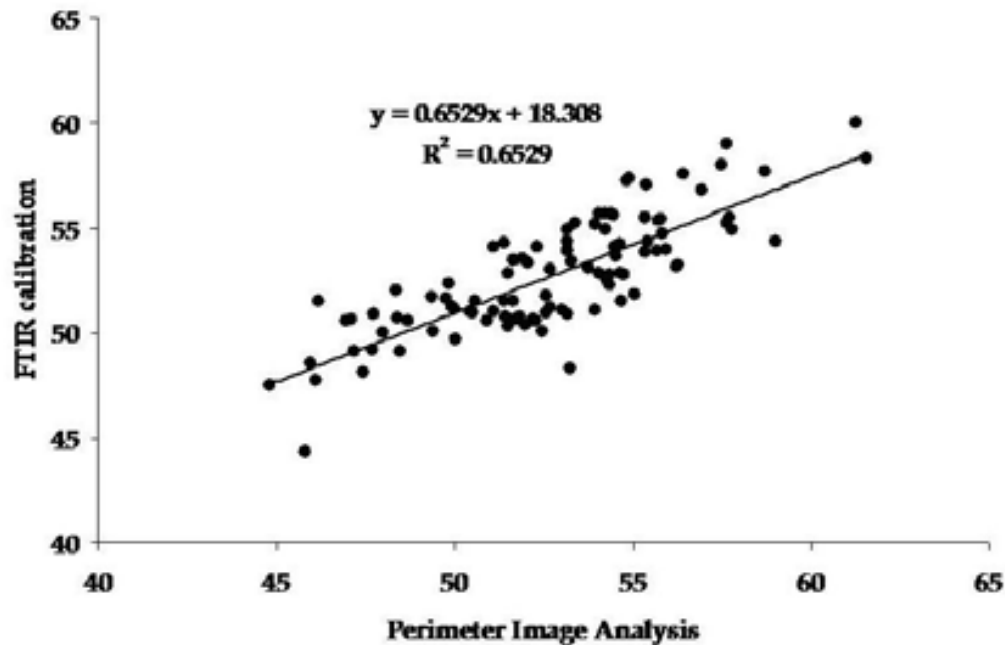


Fig. 6a. FTIR Perimeter Image Analysis prediction (calibration) versus Perimeter Image Analysis

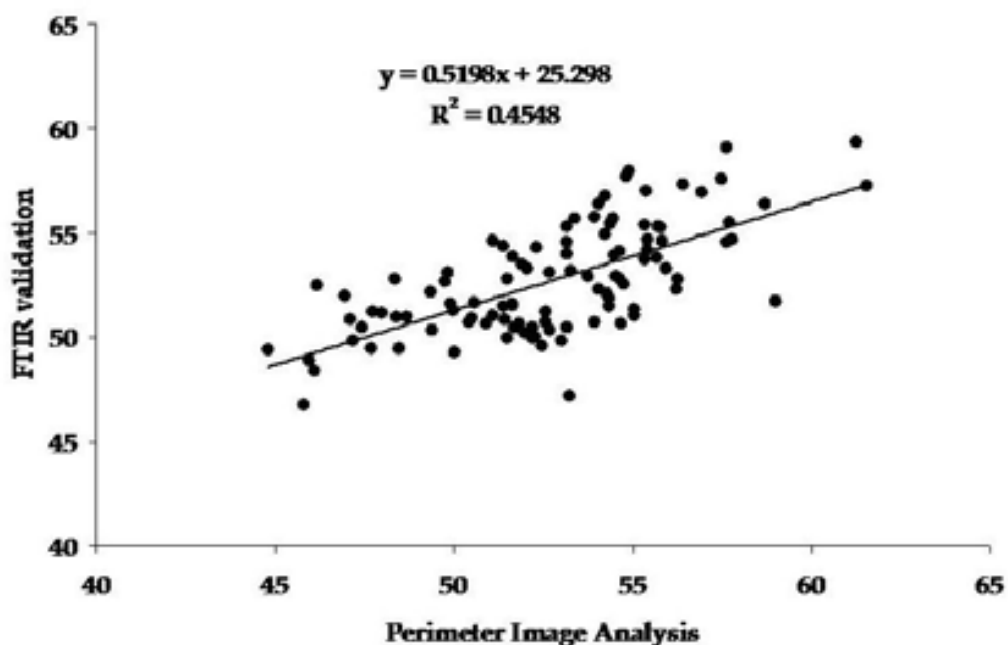


Fig. 6b. FTIR Perimeter Image Analysis prediction (validation) versus Perimeter Image Analysis

Figure 7a shows the prediction of theta (maturity) with FTIR (FTIR prediction =  $0.8107 \cdot \text{Theta} + 0.0955$ ). The coefficient of determination ( $R^2 = 0.8106$ ) of the calibration set is acceptable. However, the coefficient of determination ( $R^2 = 0.6981$ ) of the validation set is much lower than the one of the calibration set, revealing that a good prediction of maturity with this method (reflectance) is probably not possible (Fig. 7b).

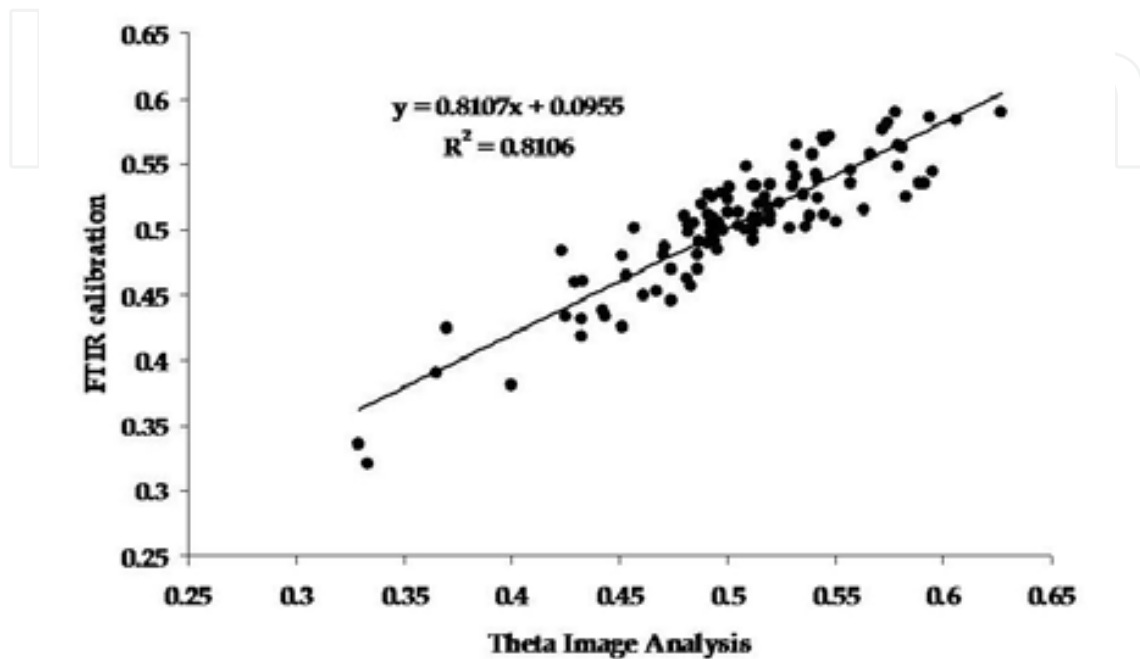


Fig. 7a. FTIR Theta Image Analysis prediction (calibration) versus Theta Image Analysis

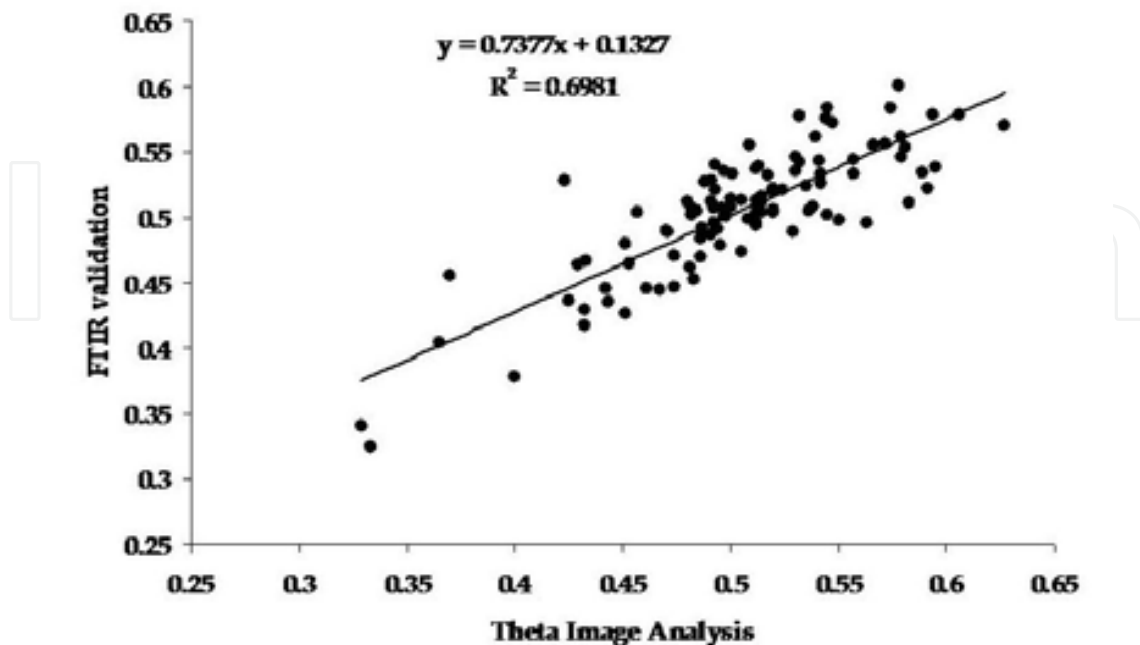


Fig. 7b. FTIR Image Analysis Theta prediction (validation) versus Theta Image Analysis

### 3.4.3 Prediction of the surface area

The results obtained with the AFIS for both Standard fineness and maturity are very similar to the one obtained with image analysis. From AFIS data, the surface area (expressed in  $\text{mm}^2/\text{mg}$ ) was calculated. Fig. 8a and b shows the prediction of the surface area by FTIR (FTIR prediction =  $0.9191 \times \text{surface area} + 26.264$ ). Both the coefficient of determination of calibration set ( $R^2 = 0.9191$ ) and the validation ( $R^2 = 0.8645$ ) are good.

Estimating the specific surface with two drastically different methods (the micronaire and the AFIS) led to the same conclusion. It is possible to predict with the FTIR the Area in  $\text{mm}^2$  per mg of fibers.

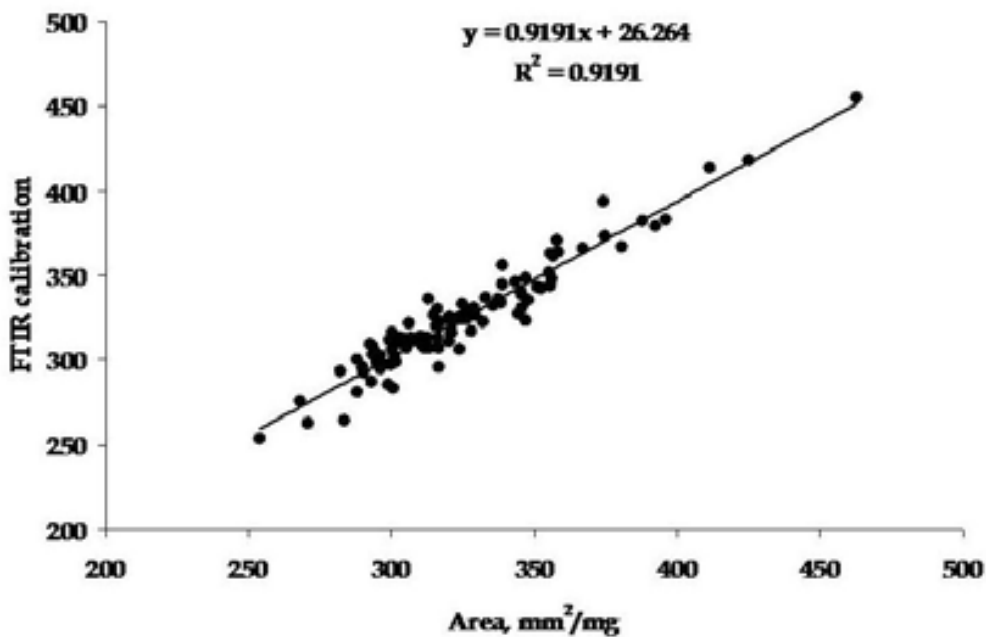


Fig. 8a. FTIR Area ( $\text{mm}^2/\text{mg}$ ) prediction (calibration) versus Area (calculated from AFIS data)

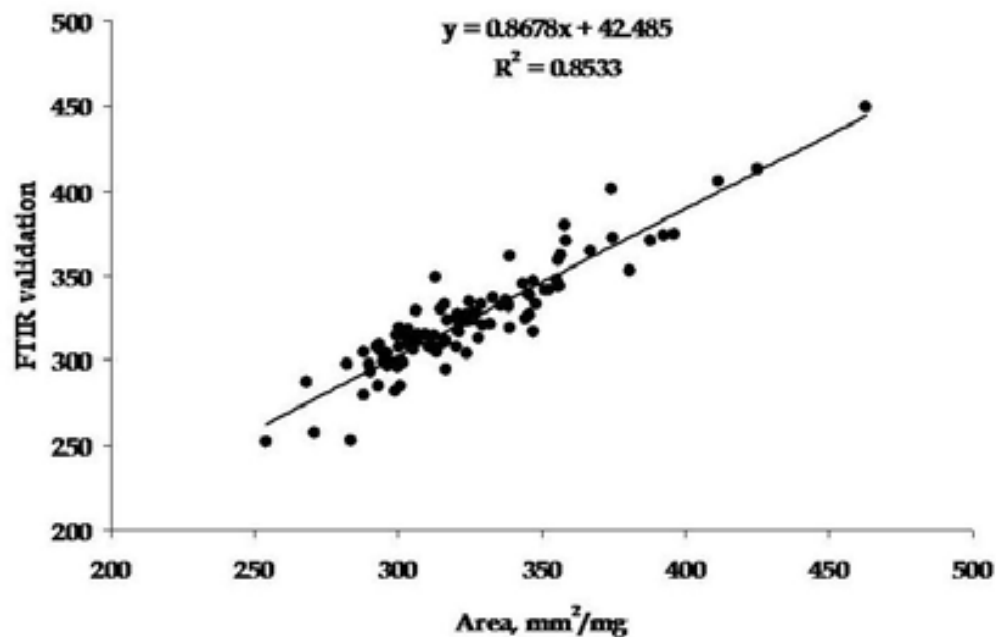


Fig. 8b. FTIR Area ( $\text{mm}^2/\text{mg}$ ) prediction (validation) versus Area (calculated from AFIS data)

### 3.5 Conclusion

In this study we investigated the use of the Universal Attenuated Total Reflectance Fourier Transform Infrared spectroscopy to evaluate the cotton fiber properties. One hundred and four cotton samples were tested and 30 FTIR spectra were acquired and analyzed from each sample. The Partial Least Square (PLS) procedure was performed on the FTIR spectra. The results showed that the micronaire and the surface area (calculated from the AFIS data) could be predicted from the FTIR measurements with very high coefficient of determination. Two drastically different techniques to estimate the surface area of the cotton fiber (micronaire and AFIS data) led to the same conclusion. However, the prediction of fiber maturity is probably not possible with FTIR because of the low coefficient of the determination. It was concluded that, to be able to predict the fiber maturity with the FTIR, it is necessary to perform the measurement in the transmission mode.

### 4. Acknowledgments

The authors would like to thank the Texas Department of Agriculture/Food and Fibers Research Grant Program, Cotton Incorporated, and the International Cotton Research Center/USDA for the financial support.

### 5. References

- Abidi, N., Hequet, E., & Ethridge, D. (2007). Thermogravimetric analysis of cotton fibers: relationships with maturity and fineness. *J Appl Polym Sci*, 103: 3476-3482
- Abidi, N., Hequet, E., Cabrales, L., Gannaway, J., Wilkins, T., & Wells, LW. (2008) Evaluating cell wall structure and composition of developing cotton fibers using Fourier transform infrared spectroscopy and thermogravimetric analysis. *J Appl Polym Sci* 107:476-486
- Carpita, NC., Defernez, M., Findlay, K., Wells, B., Shoue, DA., Catchpole, G., Wilson, RH., & McCann, MC. (2001) Cell wall architecture of the elongating Maize Coleoptile. *Plant Physiol*, 127: 551-565
- Chen, L., Carpita, NC., Reiter, W-D., Wilson, RH., Jeffries, C., & McCann, MC. (1998) A rapid method to screen for cell-wall mutants using discriminant analysis of Fourier transform spectra. *Plant J*16(3): 385-392
- Goldthwait, C.F.; Smith, H.O.; & Barnett, M.P. New dye technique shows maturity of cotton. *Textile World*, July 1947, p 105.
- Gokani, SJ., Kumar, R., & Thaker, VS. (1998). Potential Role of Abscisic Acid in Cotton Fiber and Ovule Development. *JPlant Growth Regul* 17:1-5
- Haigler, CH., Zhang, D., & Wilkerson, CG. (2005). Biotechnological improvement of cotton fibre maturity. *Physiol Plant* 124:285-294
- Hequet, E., Wyatt, B., Abidi, N., & Thibodeaux, D.P. (2006). Creation of a set of reference materials for cotton fiber maturity measurements. *Text Res J* 76(7): 576-586.
- Huwlyer, HR., Franz, G., & Meier, H. (1979). Changes in the composition of cotton fibre cell walls during development. *Planta* 146:635-642
- Hsieh, Y-L., Hu, X-P., & Nguyen, A. (1997). Strength and crystalline structure of developing Acala cotton. *Textile Res J*67(7):529-536

- Ilharco, LM., Garcia, AR., Lopez, da Silva J., & Vieira Ferreira, LF. (1997), Infrared approach to the study of adsorption on cellulose: influence of cellulose crystallinity on the adsorption of benzophenone. *Langmuir* 13:4126-4132
- Liang, C-Y., & Marchessault, RH. (1959). Infrared spectra of crystalline polysaccharides. II. Native celluloses in the region from 640 to 1700  $\text{cm}^{-1}$ . *J Polym Sci* XXXIX:269-278
- Maltby, D., Carpita, NC., Montezinos, D., Kulow, C., & Delmer, DP. (1979).  $\beta$ -1,3-glucan in developing cotton fibers, structure, localization, and relationship of synthesis to that of secondary wall cellulose. *Plant Physiol* 63:1158-1164
- McCann, MC., Chen, L., Roberts, L., Kemsley, EK., Sene, C., Carpita, NC., Stacey, NJ., & Wilson, RH. (1997). Infrared microspectroscopy: sampling heterogeneity in plant cell wall composition and architecture. *Physiol Plant* 100:729-738
- McCann, MC., Hammouri, N., Wilson, R., Belton, P., & Roberts, K. (1992). Fourier transform infrared microspectroscopy is a new way to look at plant cell walls. *Plant Physiol* 100:1940-1947
- McCann, MC., Defernez, M., Urbanowicz, BR., Tewari, JC., Langewisch, T., Olek, A., Wells, B., Wilson, RH., & Carpita, NC. (2007). Neural network analyses of infrared spectra for classifying cell wall architectures. *Plant Physiol* 143:1314-1326
- McCann, MC., Stacey, NJ., Wilson, R., & Roberts, K. (1993). Orientation of macromolecules in the walls of elongating carrot cells. *J Cell Sci* 106:1347-1356
- Meinert, MC., & Delmer, DP. (1977). Changes in biochemical composition of the cell wall of the cotton fiber during development. *Plant Physiol*. 59:1088-1097
- Montalvo, J G.& Von Hoven, T. (2004). Analysis of Cotton. In Near-Infrared Spectroscopy in Agriculture. *Agronomy Monograph* no. 44. 2004. Crop Science Society of America.
- Muller, LL. & Jacks TJ. (1975). Rapid chemical dehydration of samples for electron microscopic examinations. *JHistochem Cytochem* 23(2):107-110
- Rajasekaran, K., Muir, AJ., Ingber, BF., & French, AD. (2006). A dehydration method for immature or wet cotton fibers for light and electron microscopy. *Textile Res. J* 76(6):514-518
- Ramey, H.H. (1982) Estimating quality components of natural fibers by Near-infrared reflectance: Part 1: Cotton fiber cross-sectional area and specific surface. *Text Res J*, 52, 20-25
- Timpa, JD. & Triplett, BA. (1993). Analysis of cell-wall polymers during cotton fiber development. *Planta* 189:101-108
- Tokumoto, H., Wakabayashi, K., Kamisaka, S., & Hoson, T. (2002). Changes in the sugar composition and molecular mass distribution of matrix polysaccharides during cotton fiber development. *Plant Cell Physiol* 43(4):411-418
- Salmén, L., Åkerholm, M., & Hinterstoisser, B. (2005). Two-dimensional Fourier transform infrared spectroscopy applied to cellulose and paper. In: Dumitriu S (ed) Polysaccharides, structural diversity and functional versatility, 2nd edn. Marcel Dekker, New York, pp159-187
- Schwanninger, M., Rodrigues, JC., Pereira, H., & Hinterstoisser, B. (2004). Effects of short-time vibratory ball milling on the shape of FT-IR spectra of wood and cellulose. *Vib Spectrosc* 36:23-40
- Séné, CFB., McCann, MC., Wilson, RH., & Grinter, R. (1994). Fourier-transform Raman and Fourier-transform infrared spectroscopy an investigation of five higher plant cell walls and their components. *Plant Physiol* 106:1623-1631

- USDA, International Calibration Cotton Standards Program, USDA-AMS, Cotton Program, Memphis, TN, March 1999.
- Wilkins, TA., & Jernstedt, JA. (1999). Molecular genetics of developing cotton fibers. In: In: Basra AS (Ed) Cotton fibers, developmental biology, quality improvement, and textile processing, edn. Food Products Press, New York, pp 231-269
- Yong, W., Link, B., O'Malley, R., Tewari, J., Hunter, CT., Lu, C-An., Li, X., Bleecker, AB., Koch, KE., McCann, MC., McCarty, DR., Patterson, SE., Reiter, W-D., Staiger, C., Thomas, SR., Vermerris, W., & Carpita, NC. (2005). Genomics of plant cell wall biogenesis. *Planta* 221: 747-751



## **Fourier Transforms - New Analytical Approaches and FTIR Strategies**

Edited by Prof. Goran Nikolic

ISBN 978-953-307-232-6

Hard cover, 520 pages

**Publisher** InTech

**Published online** 01, April, 2011

**Published in print edition** April, 2011

New analytical strategies and techniques are necessary to meet requirements of modern technologies and new materials. In this sense, this book provides a thorough review of current analytical approaches, industrial practices, and strategies in Fourier transform application.

### **How to reference**

In order to correctly reference this scholarly work, feel free to copy and paste the following:

Noureddine Abidi, Eric Hequet and Luis Cabrales (2011). Applications of Fourier Transform Infrared Spectroscopy to Study Cotton Fibers, *Fourier Transforms - New Analytical Approaches and FTIR Strategies*, Prof. Goran Nikolic (Ed.), ISBN: 978-953-307-232-6, InTech, Available from:  
<http://www.intechopen.com/books/fourier-transforms-new-analytical-approaches-and-ftir-strategies/applications-of-fourier-transform-infrared-spectroscopy-to-study-cotton-fibers>

**INTECH**  
open science | open minds

### **InTech Europe**

University Campus STeP Ri  
Slavka Krautzeka 83/A  
51000 Rijeka, Croatia  
Phone: +385 (51) 770 447  
Fax: +385 (51) 686 166  
[www.intechopen.com](http://www.intechopen.com)

### **InTech China**

Unit 405, Office Block, Hotel Equatorial Shanghai  
No.65, Yan An Road (West), Shanghai, 200040, China  
中国上海市延安西路65号上海国际贵都大饭店办公楼405单元  
Phone: +86-21-62489820  
Fax: +86-21-62489821

© 2011 The Author(s). Licensee IntechOpen. This chapter is distributed under the terms of the [Creative Commons Attribution-NonCommercial-ShareAlike-3.0 License](#), which permits use, distribution and reproduction for non-commercial purposes, provided the original is properly cited and derivative works building on this content are distributed under the same license.

IntechOpen

IntechOpen